Computational Insights into Perovskite Materials: Classical Molecular Dynamics and Ab Initio Approaches

Noelia Faginas-Lago[1,3], Luca Mancini[1], Andrea Lombardi[1,3], Fernando Pirani[2], Amanda Covarelli[3(✉)], Bernardino Tirri[4], and Filippo De Angelis[1,3]

[1] Dipartimento di Chimica, Biologia e Biotecnologie, Università degli Studi di Perugia, 06123 Perugia, Italy
noelia.faginaslago@unipg.it
[2] Dipartimento di Ingegneria Civile ed Ambientale, Università degli Studi di Perugia, 06125 Perugia, Italy
[3] Istituto CNR di Scienze e Tecnologie Chimiche "Giulio Natta" (CNR-SCITEC), 06123 Perugia, Italy
amanda.covarelli@dottorandi.unipg.it
[4] Eni S.p.A, Via Emilia 1, 20097 San Donato Milanese Milan, Italy

Abstract. In the last years, Perovskite materials emerged as promising candidates for applications in photovoltaics and photocatalysis due to their exceptional optoelectronic properties, cost-effective synthesis, and structural tunability. However, their long-term stability and interaction with external molecules, such as CO_2, remain critical challenges for commercialization. In this study, we integrate classical molecular dynamics (MD) simulations and ab initio calculations to investigate the structural, electronic, and dynamical properties of perovskites. Density functional theory (DFT) is employed to optimize the geometry and compute atomic charge distributions, while MD simulations provide insights into system behavior under varying thermodynamic conditions. We preliminary analyze the role of non-covalent interactions between perovskites and CO_2 molecules, utilizing the canonical Lennard-Jones potential model. The obtained results suggest how to achieve a more accurate representation of long-range attraction and short-range repulsion, that leads to the development of refined force fields, enhancing the predictive accuracy of computational models for perovskite-based energy and environmental applications. This study lays the groundwork for future theoretical and experimental advancements aimed at optimizing perovskite materials for sustainable energy conversion and CO_2 reduction technologies.

Keywords: Perovskite · Molecular Dynamics · Ab Initio Calculations · Density Functional Theory · Non-Covalent Interactions · Photovoltaics · CO_2 Reduction · Force Field Development

© The Author(s), under exclusive license to Springer Nature Switzerland AG 2026
O. Gervasi et al. (Eds.): ICCSA 2025 Workshops, LNCS 15897, pp. 3–16, 2026.
https://doi.org/10.1007/978-3-031-97660-5_1

1 Introduction

Perovskite, originally considered the mineral name of calcium titanate (CaTiO3) [1], was discovered for the first time by Russian mineralogist Lev Perovskiy. Perovskites are used in photovoltaics because of their increasing power conversion efficiency (PCE), low-cost materials constituents, simple solution fabrication process [2], high absorption coefficient in a wide wavelength range and relatively high carrier mobility of free electrons and holes [1]. Initiated In 2009 with an efficiency of 3.8 % [2], Perovskite solar cells (PSCs) have now achieved a lab-scale power conversion efficiency of 26.7 % [3], competing with the performance of commercial silicon solar cells. Perovskites have a general chemical formula of ABX_3, where A is usually an organic cation such as methylammonium (MA) or formamidinium (FA), B is a metallic cation like tin or lead and X is an halide, such as I, Br or Cl [4]. The A-site cation is coordinated to 12 X anions, forming a cuboctahedron, while the 6-fold-coordinated B-site cation has an octahedral geometry [1], as shown in Fig. 1.

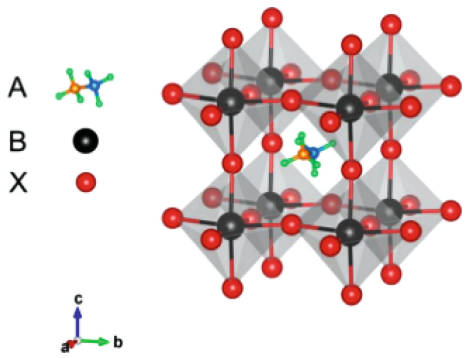

Fig. 1. Crystal structure of an organicâĂŞinorganic metal halide perovskite [5].

Tipically, PSCs have a layered device structure that includes a transparent conductive oxide (TCO)-coated glass substrate, an n-type semiconductor as the electron transport layer (ETL), a perovskite absorber layer, a p-type semiconductor as the hole transport layer (HTL), and a back-contact (metal, TCO or carbon) [2]. However, in spite of all the advantages, perovskites have a problem of stability that impedes rapid commercialization. The main issues causing instability are moisture, UV light and temperature [5]. The irreversible degradation of the perovskite layer is a problem for the lifetime of photovoltaic cells. As with multiple other solar cell technologies, also illumination with UV light can cause degradation in perovskite solar cells. Transient adsorption spectroscopy (TAS) showed that the charge collection efficiency for encapsulated perovskite cells deteriorated when exposed to UV light [5]. Exposure to elevated temperatures also causes degradation of the perovskite layer. Phillippe et al. [6] investigated

the influence of elevated temperatures on both $MAPbI_3$ and $MAPbI_{3-x}Cl_x$ films. The authors used hard X-ray photoelectron spectroscopy (XPS), rather than X-ray diffraction (XRD), to explain the film decomposition, as this allows for a determination of the chemical content regardless of the crystallinity of the sample. In this experiment, the films were heated in an analysis chamber under an ultra-high vacuum. Removing the presence of water and air allowed for the isolation of the effect of temperature on the film degradation. The films were characterised using the I/Pb and N/Pb ratios, extracted from XPS. A reduction of these ratios indicates the conversion of the perovskite into PbI_2. Heating at 100 °C for 20 min let to a significant reduction of both ratios. Further heating at 200 °C caused both ratios to drop to a minimum, 2 and 0, respectively. This is indicative of a film composed 100% of PbI_2. To overcome the stability issues, different strategies for stabilizing the active layer have been explored, including compositional engineering, controlled morphology, grain size control, perovskite deposition techniques, interfacial engineering, and many others [7]. An easy-to-implement approach is the use of additives, which in small quantities fine-tune the materials properties and increase the stability of the devices [7].

In the last years, perovskites have been considered as promising materials for different applications, including water splitting and CO_2 reduction [8]. Considering the rapid and alarming increasing of the level of atmospheric carbon dioxide, mainly due to the increase of antropic activities [9–12], photoelectrochemical CO_2 reduction represents an intriguing alternative for the reduction of the amount of CO_2, thus contributing to the field of carbon neutrality techniques. Different works have been performed to analyse and improve the efficiency of perovskites as possible catalysts for CO_2 reduction [13–18] and the actual mechanism of the process is still matter of study and debate. One of the first step of the process, which is common of all chemical processes, is represented by the long-range interaction of the CO_2 molecule with the surface of the perovskite. Such interaction will then lead to different configurations of the weakly bound precursor state of the system, which drives the species involved along specific chanels of the reactivity. Therefore, a detailed analysis of the long-range interaction and of the intermolecular forces driving the initial process can be pivotal for a better understanding of all the reactive process. In order to properly characterize the initial interaction between the two interacting species, a valid approach consists in the use of Molecular Dynamics (MD) simulations considering the appropriate range of thermodynamic conditions. As a first step, it is pivotal to implement the most accurate description of the interactions of the involved molecules through the development of a Force Field (FF), which represents a challenging task [19–21] since the choice of a correct intermolecular force field, modelling the intermolecular forces, crucially influences the realism and feasibility of the simulation studies [21]. Different functions can be used to describe the non electrostatic component of the intermolecular interaction, including the classical Lennard-Jones potential [22], but also the more accurate *Improved Lennard-Jones* (ILJ) formulation [23], which allow for a better representation of long range attraction and short range repulsion. In the present

contribution we performed preliminary MD calculation for the system composed of a perovskite layer, composed of 408 atoms in total, with 40 Pb atoms, 112 I atoms and 32 methylammonium ions ($CH_3NH_3^+$), both isolated and interacting with a CO_2 molecule using a LJ force field. The work constitutes a starting point toward the development of more accurate force field based on the physical properties of the interacting molecules.

2 Theoretical Methods

2.1 Ab Initio Calculations

Ab initio calculations have been performed at the DFT level of theory for the perovskite system. In depth, the structure of the perovskite has been optimized using the PBE functional and ultrasoft pseudopoptentials. The same computational strategy has been adopted for the optimization of the CO_2 molecule and the system composed of a carbon dioxide molecule interacting with the perovskite slab. All calculations have been performed with the Quantum Espresso package [24–26].

In order to establish the main properties of the CO_2 molecule, necessary to properly set the MD simulations, a well established computational strategy based on DFT theory has been used [27–32]. In details, the geometry has been optimized using the B3LYP functional and the aug-cc-pVTZ basis set and the atomic (Mulliken) charges have been evaluated at the same level of theory.

2.2 Molecular Dynamics

Classical molecular dynamics simulations have been performed considering both the isolated Perovskite system and the system composed of the Perovskite with a carbon dioxide molecule. In detail, the DL_POLY [33] simulation package has been used considering the NVT ensamble, where the number of particles (N), volume (V) and temperature (T) are kept constant. For this purpose, a Hoover-Nose thermostat [34] has been used, with a relaxation constant of 1 ps. Parallelepiped boundary conditions have been used, considering the shape and dimensions commisurated with the unit cell of the structure (see Sect. 3 for details). NVT simulations have been performed considering a temperature of 300 K and a pressure of 1 atm. An initial equilibration period of 1 ns has been performed, considering a total simulation time of 3 ns.

2.3 Non-covalent Interactions: Potential Energy Surface

In order to obtain a reliable Force Field to be used in the simulation, the global intermolecular interaction energy (V_{Tot}) has been considered as a combination of an electrostatic contribution (V_{Elec}) and a non-electrostatic contribution (V_{Nelec}):

$$V_{Tot} = V_{Elec} + V_{Nelec} \tag{1}$$

where the electrostatic contribution has been calculated taking into account the atomic charge distribution of the system, evaluated at the DFT level of theory and reported in Table 1. In the case of the CO_2 molecule, the atomic charges reported in Fig. 7 are consistent with the electric molecular quadrupole (Fig. 2).

Table 1. Average atomic (Mulliken) charges calculated for the structure reported in Fig. 3.

Atom	Charge
Pb	+0.317
I	–0.339
N	+0.282
C	–0.222
H	+0.112

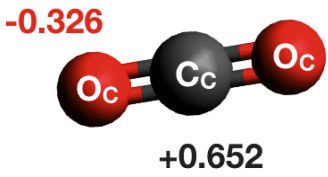

Fig. 2. Atomic charges evaluated for the CO_2 molecule.

The non-electrostatic component of the intermolecular interaction has been evaluated considering the *Lennard-Jones* formulation [22]. The LJ potential model for a pair of neutral particles can be formulated as follows:

$$V_{LJ} = 4\varepsilon\left[\left(\frac{\sigma}{r}\right)^{12} - \left(\frac{\sigma}{r}\right)^{6}\right] \tag{2}$$

where σ represents the intermediate distance where the potential V goes to zero. Moreover, the long-range attraction coefficient is defined as:

$$C_6 = 4\varepsilon\sigma^6 \tag{3}$$

In this model, the potential well, describing the intermolecular binding energy and its characteristics arise from a balance between attraction and repulsion forces. Despite the simplicity of the formulation, the LJ model is still widely used in molecular dynamics simulations today due to its simplicity, exportability and differentiability of the adopted function. The pair parameters, obtained starting from literature values [35–37], were evaluated considering the combination rules

proposed initially by Lorentz and Berthelot [38,39] are reported in Table 2 for the Perovskite system, while in Table 3 are reported the parameters for the Perovskite - CO_2 interaction.

Table 2. List of the Lennard-Jones parameters evaluated for the Perovskite system.

Interacting Pair	σ (Å)	ε (kcal)
Pb - Pb	3.188	0.1015
Pb - I	2.884	0.1387
Pb - C	3.604	0.0118
Pb - N	3.524	0.0174
Pb - H	2.124	0.0084
I - I	2.580	0.0108
I - C	3.300	0.0039
I - N	3.220	0.0057
I - H	1.820	0.0027
C - N	3.940	0.0020
C - H	2.540	0.00096
N - N	3.860	0.0029
N - H	2.460	0.0014
H - H	1.060	0.00069

Table 3. List of the Lennard-Jones parameters evaluated for the Perovskite - CO_2 system.

Interacting Pair	σ (Å)	ε (kcal)
Pb - C_C	2.969	0.0106
Pb - O_C	3.109	0.0193
I - C_C	2.660	0.0037
I - O_C	2.805	0.0063
N - C_C	3.305	0.0019
N - O_C	3.445	0.0033
C - C_C	3.385	0.0013
C - O_C	3.525	0.0022
H - C_C	1.905	0.00094
H - O_C	2.045	0.0015

3 Results and Discussion

The global Perovskite system used in the present work is composed of four layers with a total of 408 atoms, including 40 Pb atoms, 112 I atoms and 32 methylammonium ions ($CH_3NH_3^+$), which can be considered as a good prototype for the lead halide perovskite [40] The global structure is reported in Fig. 3. As can be seen from the representation reported in the figure, the structure of the perovskite is composed by five layers in which lead and iodine atoms form an octahedral structure, generating spaces which are occupied by methylammonium cations.

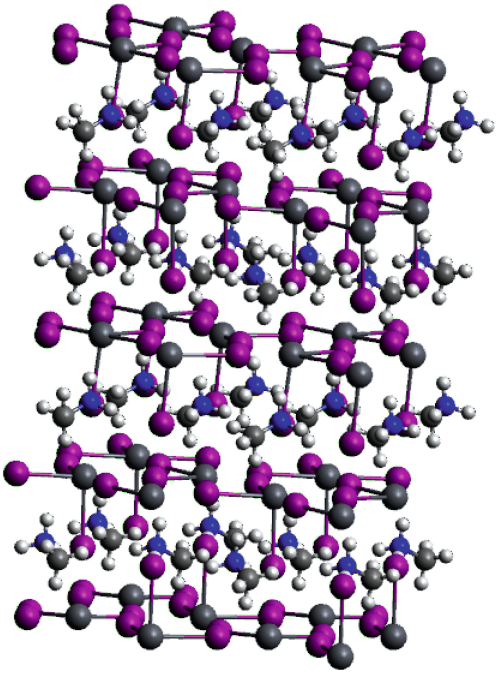

Fig. 3. 3D representation of the structure of the Perovskite used for the present analysis.

In order to run a proper MD simulation, it is pivotal to set appropriate values for the periodic boundary conditions, and, therefore, to analyze the accurate unit cell to be repeated during the simulation. In the present case, as reported also in Sect. 2, parallelepiped boundary conditions have been used, considering a unit cell whose dimensions are $9 \times 9 \times 13$ Å. A schematic representation of the unit cell used for the preliminary MD calculations is reported in Fig. 4.

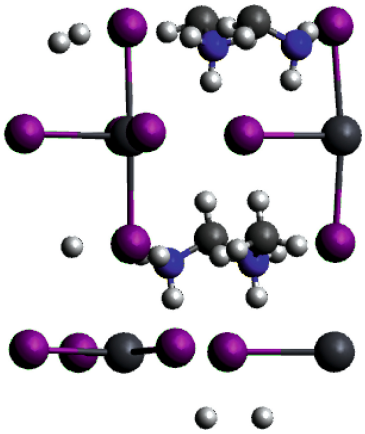

Fig. 4. Unit cell used for the calculations.

An initial analysis has been performed considering only the perovskite system, in order to set the ideal simulation environment and check the stability of the simulation. In Figs. 5 and 6 are reported the trends of the Total Energy and Temperature as a function of the simulation time.

As can be seen, the fluctuations of energy and temperature during the MD calculations are considerably small with respect to the absolute value, thus indicating the goodness of the simulation parameters adopted.

After the initial assessment of the simulation parameters, a new analysis was performed considering the interaction of a CO_2 molecule with the perovskite. An initial *ab initio* analysis was carried out (see Sect. 2 for details) considering a relaxation (optimization) procedure where the first three layers from the bottom of the perovskite structure (along the z-axis)are kept rigid, while the last two layers, which are closer to the CO_2 molecule, are able to relax. The same strategy has been used for both the isolated perovskite and the perovskite interacting with the CO_2 molecule. The resulting strucure, obtained through *ab initio* calculations, is reported in Fig. 7

The energy of the system can be easily calculated, allowing to quantify the strength of the interaction between the CO_2 molecule in the gas phase and the surface of the perovskite. In details, the adsorption energy can be evaluated as follows:

$$E_{ads} = E_{tot} - E_{per} - E_{\mathrm{CO_2}} \tag{4}$$

where E_{tot} is the energy deriving from the optimized structure of the perovskite with the CO_2 molecule, while E_{per} and E_{CO_2} represent the energies of the perovskite and CO_2 optimized separately, obtained at the DFT level of theory. Following the formulation reported in Eq. 4, a value of E_{ads} = –5.07 kcal/mol was obtained. The value can be compared with the results derived from a preliminary MD analysis, performed considering a *Lennard-Jones* formulation of

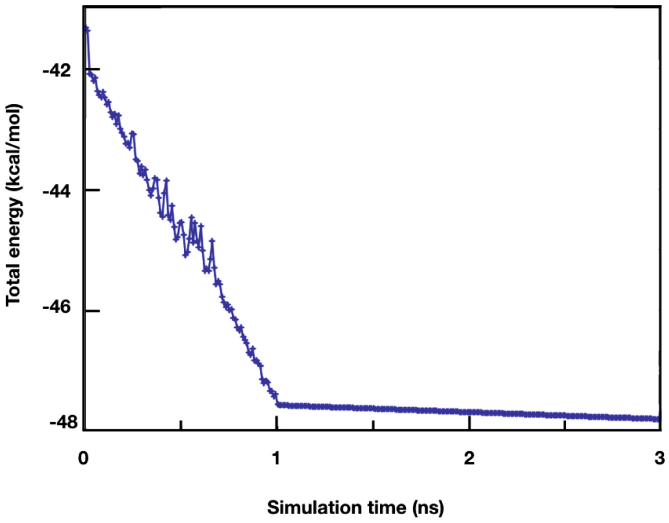

Fig. 5. Trend of the total energy (in kcal/mol) as a function of the simulation time (ns) for the Perovskite system, obtained through MD calculations.

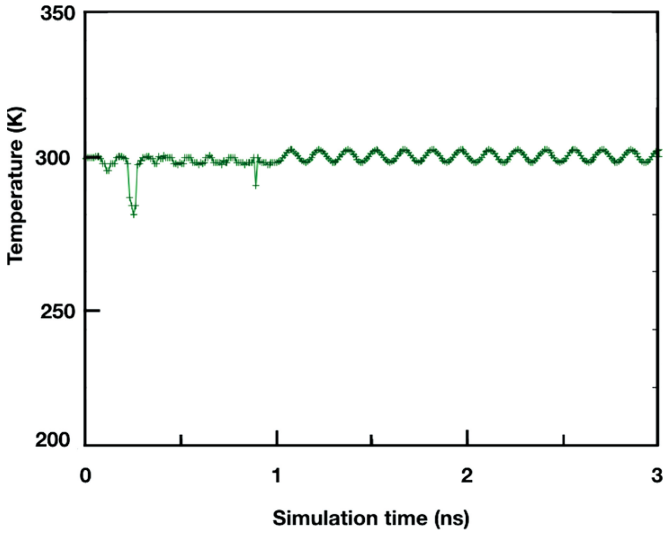

Fig. 6. Trend of the temperature (in K) as a function of the simulation time (ns) for the Perovskite system.

the non-electrostatic interaction (see Table 3 for details). Also in this case, the interaction energy was evaluated considering the difference between the configurational energy of the perovskite+CO_2 system and the configurational energy of the two interacting species, calculated separately. The value obtained from clas-

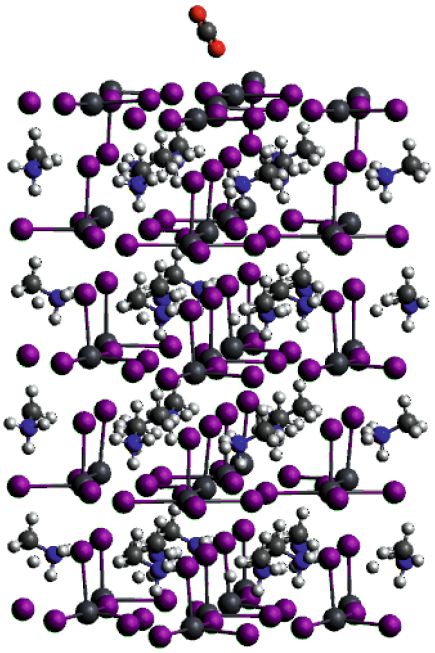

Fig. 7. 3D representation of the structure of the perovskite system interacting with a CO_2 molecule.

sical MD calculation is equal to –3.54 kcal/mol, differing of around 1.5 kcal/mol with respect to the value coming from *ab initio* calculations. An additional analysis can be performed considering the geometry resulting from *ab initio* calculations, and in particular taking into account the distance between the CO_2 molecule and the Perovskite layer. In Table 4 are reported the main distances obtained through accurate *ab initio* calculations.

The results reported in Table 4 can be directly compared with the σ parameters of the LJ formulation (see Table 3). As can be seen, the main interaction distances estimated using the Lennard-Jones formulation are considerably lower than the ones obtained from the *ab initio* calculations. The most important deviation can be appreciated considering the I-C−C interaction, where the difference is around 2 . One of the reasons of the disagreement between accurate *ab initio* calculations and classical molecular dynamics simulations can be attributed to the force field adopted for the simulations. In particular, a different formulation of both the electrostatic and the non-electrostatic potential can be used to properly take into account the effect of the chemical environment in the description of the atom-atom interactions. For this purpose, the *Improved Lennard-Jones* [23] formulation of the potential can be of great help, since the main parameters governing the interactions are related to fundamental physical quantities, such as charge distribution and atomic/moleculear polarizabilities. In order to have a proper representation of all the interaction centers with a limited computational

Table 4. Atom-atom distances (in Å) between the CO_2 molecule and the first layer of the perovskite structure, obtained through DFT calculations (see Sect. 2.1 for details).

Interacting Pair	dist. (Å)
C_C - Pb	4.021
O_C - I	2.996
C_C - Pb	4.628
O_C - I	4.188

cost, in the case of complex systems, it can be necessary to consider different moieties globally as effective atoms, each one having polarizability equal to the average molecular component, in order to provide a simplified formulation of the multidimensional Potential Energy Surface (PES).

4 Conclusions

In the present contribution, we performed a preliminary molecular dynamics (MD) analysis of the interaction between CO_2 and perovskites, using the canonical Lennard-Jones potential function to model the non-covalent interactions. The obtained results were compared with high level *ab initio* calculations, to evaluate the quality of the results. The obtained results show a slight disagreement between classical MD simulations and *ab initio* resulting, suggest that the initial force field needs to be adjusted to better represent the non-covalent interactions. A first refinement can be done modeling the electrostatic contribution considering a different charge distribution on the perovskite, where the atomic charges are +2 for the Pb atoms, –1 for the I and +1 for the CH_3NH_3 cation. Additionally, in order to achieve a more accurate representation of long-range attraction and short-range repulsion, a different computational models can be used, namely the *Improved Lennard-Jones* formulation, where the parameters are linked to physical properties, such as dipole moment and electric dipole. The present study lays the basis of a future characterization, allowing to properly represent the interaction between perovskyte systems and small molecules, with particular relevance in the field of energy storage.

Acknowledgments. This work has been funded by the European Union - NextGenerationEU under the Italian Ministry of University and Research (MUR) National Innovation Ecosystem grant ECS00000041 - VITALITY - CUP J97G22000170005. N.F.L, A.L. and F. DA acknowledge funding by the Italian Ministry of Environment and Energy Security in the framework of the Project GoPV (CSEAA_00011) for Research on the Electric System. A.C., from UniPG, acknowledges the financial support of Eni S.p.A. for research activities conducted within the PhD cycle XXXIX.

Disclosure of Interests. The authors have no competing interests to declare that are relevant to the content of this article.

References

1. Kim, J.Y., Lee, J.W., Jung, H.S., Shin, H., Park, N.G.: High-efficiency perovskite solar cells. Chem. Rev. **120**(15), 7867–7918 (2020)
2. Rong, Y., et al.: Challenges for commercializing perovskite solar cells. Science **361**(6408), eaat8235 (2018)
3. Mao, L., Xiang, C.: A comprehensive review of machine learning applications in perovskite solar cells: materials discovery, device performance, process optimization and systems integration. Mater. Today Energy, 101742 (2024)
4. Correa-Baena, J.P., et al.: Promises and challenges of perovskite solar cells. Science **358**(6364), 739–744 (2017)
5. Wang, D., Wright, M., Elumalai, N.K., Uddin, A.: Stability of perovskite solar cells. Sol. Energy Mater. Sol. Cells **147**, 255–275 (2016)
6. Philippe, B., Park, B.W., Lindblad, R., Oscarsson, J., Ahmadi, S., Johansson, E.M., Rensmo, H.: Chemical and electronic structure characterization of lead halide perovskites and stability behavior under different exposures a photoelectron spectroscopy investigation. Chem. Mater. **27**(5), 1720–1731 (2015)
7. Valero, S., Soria, T., Marinova, N., Delgado, J.L.: Efficient and stable perovskite solar cells based on perfluorinated polymers. Polym. Chem. **10**(42), 5726–5736 (2019)
8. Bienkowski, K., et al.: Halide perovskites for photoelectrochemical water splitting and co2 reduction: challenges and opportunities. ACS Catal. **14**(9), 6603–6622 (2024)
9. Harfoot, M.B., et al.: Present and future biodiversity risks from fossil fuel exploitation. Conserv. Lett. **11**(4), e12448 (2018)
10. Deutz, S., et al.: Cleaner production of cleaner fuels: wind-to-wheel-environmental assessment of co_2-based oxymethylene ether as a drop-in fuel. Energy Environ. Sci. **11**(2), 331–343 (2018)
11. Marques, A.C., Fuinhas, J.A., Pereira, D.A.: Have fossil fuels been substituted by renewables? An empirical assessment for 10 European countries. Energy Policy **116**, 257–265 (2018)
12. Rogelj, J., et al.: Scenarios towards limiting global mean temperature increase below 1.5 c. Nat. Climate Change **8**(4), 325–332 (2018)
13. Tang, C., Chen, C., Xu, W., Xu, L.: Design of doped cesium lead halide perovskite as a photo-catalytic co 2 reduction catalyst. J. Mater. Chem. A **7**(12), 6911–6919 (2019)
14. Shyamal, S., Pradhan, N.: Halide perovskite nanocrystal photocatalysts for co2 reduction: successes and challenges. J. Phys. Chem. Lett. **11**(16), 6921–6934 (2020)
15. Chen, J., Dong, C., Idriss, H., Mohammed, O.F., Bakr, O.M.: Metal halide perovskites for solar-to-chemical fuel conversion. Adv. Energy Mater. **10**(13), 1902433 (2020)
16. Zhang, X., Tang, R., Li, F., Zheng, R., Huang, J.: Tailoring inorganic halide perovskite photocatalysts toward carbon dioxide reduction. Solar RRL **6**(6), 2101058 (2022)
17. Yuan, J., Liu, H., Wang, S., Li, X.: How to apply metal halide perovskites to photocatalysis: challenges and development. Nanoscale **13**(23), 10281–10304 (2021)
18. Chen, S., Yin, H., Liu, P., Wang, Y., Zhao, H.: Stabilization and performance enhancement strategies for halide perovskite photocatalysts. Adv. Mater. **35**(6), 2203836 (2023)

19. Marques, J., et al.: A global optimization perspective on molecular clusters. Phil. Trans. R. Soc. A: Math. Phys. Eng. Sci. **375**(2092), 20160198 (2017)
20. Cappelletti, D., Falcinelli, S., Pirani, F.: The dawn of hydrogen and halogen bonds and their crucial role in collisional processes probing long-range intermolecular interactions. Phys. Chem. Chem. Phys. **26**, 7971–7987 (2024)
21. Marques, J.M., Prudente, F.V., Pirani, F.: Intermolecular forces: from atoms and molecules to nanostructures (2022)
22. Lennard-Jones, J., Hall, G.: Je lennard-jones proc. Roy. Soc. Lond. A. **106**, 441 (1924)
23. Pirani, F., Brizi, S., Roncaratti, L.F., Casavecchia, P., Cappelletti, D., Vecchiocattivi, F.: Beyond the lennard-jones model: a simple and accurate potential function probed by high resolution scattering data useful for molecular dynamics simulations. Phys. Chem. Chem. Phys. **10**(36), 5489–5503 (2008)
24. Giannozzi, P., et al.: Quantum espresso: a modular and open-source software project for quantum simulations of materials. J. Phys. Conden. Matt. **21**(39), 395502 (2009). http://www.quantum-espresso.org
25. Giannozzi, P., et al.: Advanced capabilities for materials modelling with quantum espresso. J. Phys. Conden. Matter **29**(46), 465901 (2017). http://stacks.iop.org/0953-8984/29/i=46/a=465901
26. Giannozzi, P., et al.: Quantum espresso toward the exascale. J. Chem. Phys. **152**(15), 154105 (2020)
27. Pannacci, G., et al.: A combined crossed molecular beam and theorerical study of the O(^{3}P, ^{1}D) + acrylonitrile (CH_2CHCN) reactions and implications for combustion and extraterrestrial environments. Phys. Chem. Chem. Phys. **25**(30), 20194–20211 (2023)
28. Liang, P., et al.: Oh (2π)+ c2h4 reaction: a combined crossed molecular beam and theoretical study. J. Phys. Chem. A **127**(21), 4609–4623 (2023)
29. Rosi, M., et al.: Electronic structure and kinetics calculations for the Si+SH reaction, a possible route of SiS formation in star-forming regions. In: Misra, S., et al. (eds.) ICCSA 2019. LNCS, vol. 11621, pp. 306–315. Springer, Cham (2019). https://doi.org/10.1007/978-3-030-24302-9_22
30. Liang, P., et al.: Combined crossed molecular beams and computational study on the n (2d)+ hcccn (x1σ+) reaction and implications for extra-terrestrial environments. Mol. Phys. **120**(1–2), e1948126 (2022)
31. Vanuzzo, G., et al.: The n (2d)+ ch2chcn (vinyl cyanide) reaction: a combined crossed molecular beam and theoretical study and implications for the atmosphere of titan. J. Phys. Chem. A **126**(36), 6110–6123 (2022)
32. Vanuzzo, G., Mancini, L., Pannacci, G., Liang, P., Marchione, D., Recio, P., Tan, Y., Rosi, M., Skouteris, D., Casavecchia, P., et al.: Reaction n (2d)+ ch2cch2 (allene): an experimental and theoretical investigation and implications for the photochemical models of titan. ACS Earth Space Chem. **6**(10), 2305–2321 (2022)
33. Smith, W., Yong, C., Rodger, P.: Dl_poly: application to molecular simulation. Mol. Simul. **28**(5), 385–471 (2002)
34. Hoover, W.G.: Canonical dynamics: equilibrium phase-space distributions. Phys. Rev. A **31**(3), 1695 (1985)
35. Poling, B.E., Prausnitz, J.M., O'connell, J.P., et al.: The Properties of Gases and Liquids, vol. 5. Mcgraw-hill, New York (2001)
36. Maghfiroh, C.Y., Arkundato, A., Maulina, W., et al.: Parameters (σ, ε) of lennard-jones for fe, ni, pb for potential and cr based on melting point values using the molecular dynamics method of the lammps program. In: Journal of Physics: Conference Series. vol. 1491, p. 012022. IOP Publishing (2020)

37. Freindorf, M., Shao, Y., Furlani, T.R., Kong, J.: Lennard-jones parameters for the combined qm/mm method using the b3lyp/6-31g*/amber potential. J. Comput. Chem. **26**(12), 1270–1278 (2005)
38. Lorentz, H.: About the application of the virial theorem in the kinetic theory of gases. Ann. Phys. **248**(1), 127–136 (1881)
39. Berthelot, D., Amoreux, G.: Comptes rendus acad (1898)
40. Canil, L., et al.: Halogen-bonded hole-transport material suppresses charge recombination and enhances stability of perovskite solar cells. Adv. Energy Mater. **11**(35), 2101553 (2021)